



## Imidazo[1,2-*a*]pyrazines as novel PI3K inhibitors

Sonia Martínez González, Ana Isabel Hernández, Carmen Varela, Sonsoles Rodríguez-Arístegui, Rosa María Álvarez, Ana Belén García, Milagros Lorenzo, Virginia Rivero, Julen Oyarzabal<sup>†</sup>, Obdulia Rabal<sup>‡</sup>, James R. Bischoff<sup>‡</sup>, Maribel Albarrán, Antonio Cebriá, Patricia Alfonso, Wolfgang Link, Jesús Fominaya, Joaquín Pastor<sup>\*</sup>

Experimental Therapeutics Program, Spanish National Cancer Research Centre (CNIO). C/Melchor Fernández Almagro 3, E-28029 Madrid, Spain

### ARTICLE INFO

#### Article history:

Received 9 December 2011

Revised 18 January 2012

Accepted 20 January 2012

Available online 28 January 2012

#### Keywords:

PI3K inhibitors

p110  $\alpha, \beta, \delta, \gamma$

8-Morpholinyl Imidazo[1,2-*a*]pyrazines

Cancer treatment

### ABSTRACT

Phosphoinositide-3-kinase (PI3K) is an important target for cancer therapeutics due to the deregulation of its signaling pathway in a wide variety of human cancers. We describe herein a novel series of imidazo[1,2-*a*]pyrazines as PI3K inhibitors.

© 2012 Elsevier Ltd. All rights reserved.

The lipid phosphoinositide 3-kinase (PI3K) is a central component in the PI3K/AKT/mTOR signaling pathway. This enzyme catalyzes phosphorylation of the 3-hydroxyl position of phosphatidylinositides (PIs) and plays a crucial role in mitogenic signal transduction.<sup>1–4</sup> Various subtypes of PI3K have been identified to date,<sup>5–8</sup> Class Ia PI3Ks (p110 $\alpha$ , p110 $\beta$ , and p110 $\delta$ ), activated by tyrosine kinase receptors, are known to play critical roles in cell growth and survival.<sup>9</sup> Class Ib has one family member, p110 $\gamma$ . It is activated directly by G protein-coupled receptors and linked mainly with inflammatory, allergic responses, transcription and translation.<sup>10,11</sup>

All four isoforms of PI3K have different distributions and share similar cellular functions, which are context dependent. They seem to be implicated in various degrees in the development of cancer and are often up-regulated and mutated in cancer cells. In particular, in ovarian, breast, colon, and brain cancers, p110 $\alpha$  is often up-regulated, by overexpression, gene amplification, mutation, and/or PTEN phosphatase deletion.<sup>12–15</sup> It also contributes to acquired resistance to both targeted anticancer therapies and conventional cytotoxic agents.<sup>16–20</sup> On the other hand, the kinase activity of p110 $\beta$  is essential in cellular transformation caused by PTEN loss.<sup>21</sup>

It is important to mention that the expression of PI3K $\delta$  is confined to leukocytes, playing a key role in cell survival in leukaemia and other haematological malignancies.<sup>22,23</sup>

Based on these precedents, PI3K has emerged as an attractive target for the discovery of cancer therapeutics and several groups are working to identify potent small molecule inhibitors of this signaling pathway.

A considerable number of PI3K inhibitors described in the literature contains a 'morpholinyl-pyrimidine' substructure (Fig. 1); some of them (e.g., BKM-120<sup>24</sup> and GDC-0941<sup>25</sup>) are currently under evaluation in human clinical trials.

In order to find new hits for our PI3K program, we carried out, in parallel, a HTS campaign together with a rational design exercise based on known PI3K inhibitors structures. The results of the HTS and the exploration of the corresponding hits have been previously reported.<sup>26</sup> We would now like to report our findings using the latter strategy.

The replacement of the central core in bioactive molecules is a common practice in medicinal chemistry to find proprietary and novel hits. As we mentioned before, the 'morpholinyl-pyrimidine' substructure as part of monocyclic (e.g., BKM-120)<sup>24</sup>, bicyclic (e.g., PI-249)<sup>27</sup> or tricyclic (e.g., PI-103)<sup>28</sup> PI3K inhibitors, has been widely used.<sup>29</sup> In particular, for bicyclic and tricyclic inhibitors, the junctions between the pyrimidine ring and the fused cycle were always defined by a C–C unit (i.e., C<sub>4a</sub>–C<sub>7a</sub> in PI-249 and GDC-0941). In this context, the design of bicyclic compounds bearing an N atom in bridgehead position was less obvious, and could

\* Corresponding author. Tel.: +34 917328000; fax: +34 917328051.

E-mail address: [jpastor@cnio.es](mailto:jpastor@cnio.es) (J. Pastor).

<sup>†</sup> Present address: Center for Applied Medical Research (CIMA), Small Molecule Discovery, Avda. Pio XII, 31008 Pamplona, Spain.

<sup>‡</sup> Johnson & Johnson Pharmaceutical R&D, 2340 Beerse, Belgium.

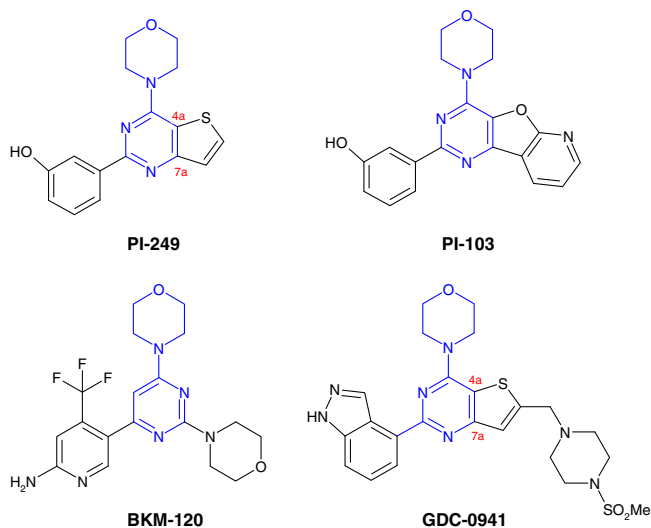


Figure 1. Chemical structures of PI3K inhibitors.

Table 1  
Inhibition of PI3K $\alpha$  by imidazo[1,2-*a*]pyrazine derivatives<sup>a</sup>

Compound	R <sup>2</sup>	R <sup>3</sup>	PI3K (p110 $\alpha$ ) IC <sub>50</sub> , $\mu$ M
1	H	H	0.197
2	Me	H	0.096
3	Cyclopropyl	H	0.340
4	CF <sub>3</sub>	H	0.108
5	CH <sub>2</sub> OH	H	0.639
6		H	0.444
7		H	2.75
8		H	0.451
9		H	0.037
10		H	0.540
11	H		0.512
12	H		0.897
13	H		0.526

<sup>a</sup> The values are averages of two independent experiments performed in duplicate with typical variation of less than  $\pm 20\%$ . Assay conditions are described in Ref. 37.

potentially afford novel inhibitors. We describe herein the design and preparation of a novel series of imidazo[1,2-*a*]pyrazine PI3K inhibitors.

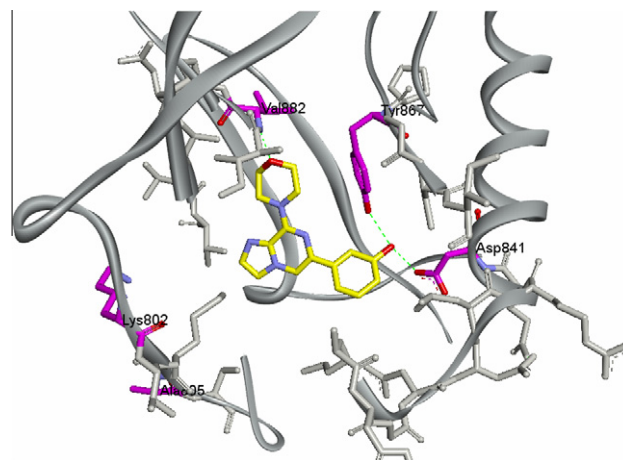


Figure 2. Proposed binding mode of compound 1 in PI3K $\gamma$ .

In order to evaluate the potential of this novel PI3K scaffold, we synthesized a couple of imidazo[1,2-*a*]pyrazine probes, compounds 1 and 2 (Table 1), which showed an activity against p110 $\alpha$  of 197 and 96 nM, respectively. Both compounds incorporate two fragments, morpholinyl and 3-hydroxyphenyl, that play an important role in their binding with PI3K.<sup>25,27,30,31</sup>

The proposed binding mode of these compounds in p110 $\gamma$  is shown in Figure 2. The model was built in p110 $\gamma$  based on the high homology between the  $\alpha$  and  $\gamma$  isoforms in the catalytic site, so a similar binding mode was then expected. The morpholine oxygen would form a hydrogen bond to the hinge Val882 NH. The phenol hydroxyl group would make hydrogen bonds with Asp841 and Tyr867 residues of PI3K $\gamma$ .

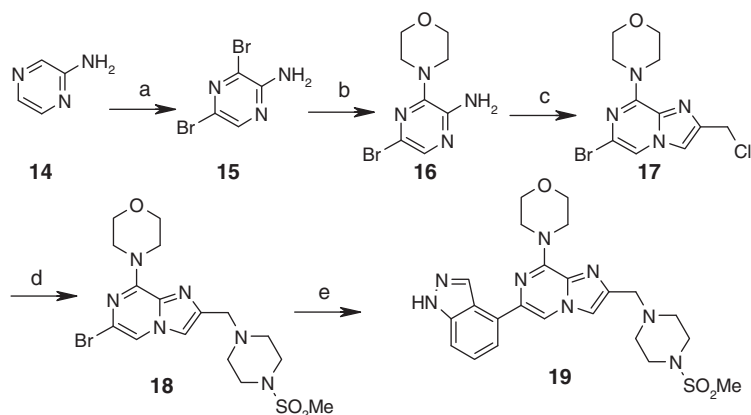
The C<sub>2</sub>–C<sub>3</sub> positions of these structures extend out toward the so called solvent accessible area in PI3K. The exploration of this region was achieved by substitution with different R<sup>2</sup>, R<sup>3</sup> fragments, including 4-methanesulfonyl-piperazin-1-ylmethyl group, present in GDC-0941, with reported hydrogen bond interactions to Lys802 and Ala805.<sup>25</sup> Selected results of this exploration are shown in Table 1.

Compounds 4 and 9 displayed activity values in PI3K $\alpha$  better or in the same range than our initial hits (1,2). However, other modifications at C<sub>2</sub> gave less active inhibitors. Substitution of C<sub>3</sub> with secondary amines yielded compounds 11–13, with lower inhibitory activity (0.5–1  $\mu$ M).

Among these derivatives, compound 9 showed to be the most potent inhibitor (IC<sub>50</sub> PI3K $\alpha$ : 37 nM). However, its in vivo potential was limited by the presence of the metabolically unstable 3-hydroxyphenyl group. In order to overcome this issue, we replaced this fragment by the known isosteric indazole, following a similar strategy to that applied by the Genentech team for the optimization of GDC-0941.<sup>25</sup>

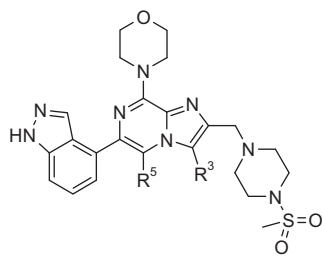
The synthesis of compound 19, within the imidazo[1,2-*a*]pyrazine series is depicted in Scheme 1. Bromination of 2-aminopyrazine 14, followed by morpholine introduction gave pyrazine 16. The condensation with 1,3-dichloroacetone yielded chloride 17, which reacted with *N*-mesyloxy-piperazine to give precursor 18. Finally, Suzuki–Miyaura cross coupling with indazol-4-boronic acid afforded the target compound.

Indazole derivative 19 was potent, IC<sub>50</sub> PI3K $\alpha$ : 95 nM, but 2.5-fold less active against PI3K $\alpha$  than the 3-hydroxyphenyl counterpart 9. Additionally, it was 30 times less active than the benchmark GDC-0941 (3.0 nM).<sup>25</sup> When we introduced a bromine atom in C<sub>3</sub>, the inhibitory activity towards PI3K $\alpha$  was improved 2-fold (20), meanwhile exploration of C<sub>5</sub> with small groups such as chlorine and cyano (21,22) produced a slight decrease in



**Scheme 1.** Reagents and conditions: (a)  $\text{Br}_2$ , Py,  $\text{CHCl}_3$ , rt 36%; (b) morpholine, 120 °C, 96%; (c) 1,3-dichloroacetone,  $i\text{PrOH}$ , 60 °C, 38%; (d) *N*-Ms-piperazine,  $\text{K}_2\text{CO}_3$ ,  $\text{CH}_3\text{CN}$ , 100 °C, 90%; (e)  $\text{PdCl}_2(\text{dppf})\text{DCM}$ , aq.  $\text{K}_2\text{CO}_3$ , indazole-4-boronic acid hydrochloride, DME, 130 °C, 75%.

**Table 2**  
Inhibition of PI3K $\alpha$  and phosphorylation of AKT by imidazo[1,2-*a*]pyrazine derivatives<sup>a</sup>



Compound	R <sup>3</sup>	R <sup>5</sup>	PI3K(p110 $\alpha$ ) IC <sub>50</sub> , $\mu\text{M}$	pAKT EC <sub>50</sub> , $\mu\text{M}$
<b>19</b>	H	H	0.095 ± 0.016	0.093 ± 0.031
<b>20</b>	Br	H	0.047 ± 0.009	0.208 ± 0.072
<b>21</b>	H	CN	0.194 ± 0.018	0.203 ± 0.069
<b>22</b>	H	Cl	0.145 ± 0.021	0.495 ± 0.099

<sup>a</sup> The values are averages of two independent experiments performed in duplicate ± Standard Deviation. Assay conditions are described in Ref. 37,38.

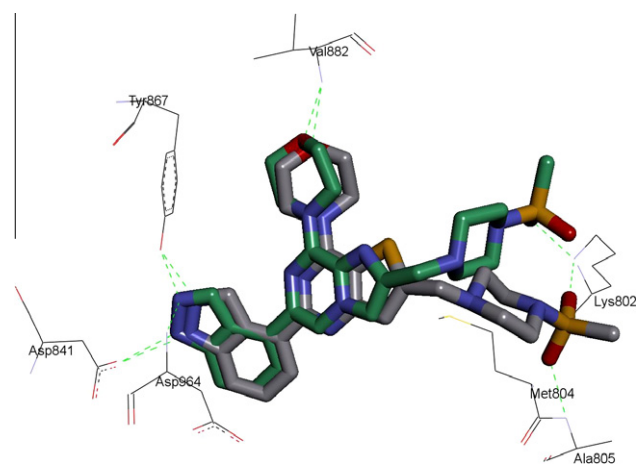


**Figure 3.** Overlay of GDC-0941 (grey) and compound **19** (green) in PI3K $\gamma$ .

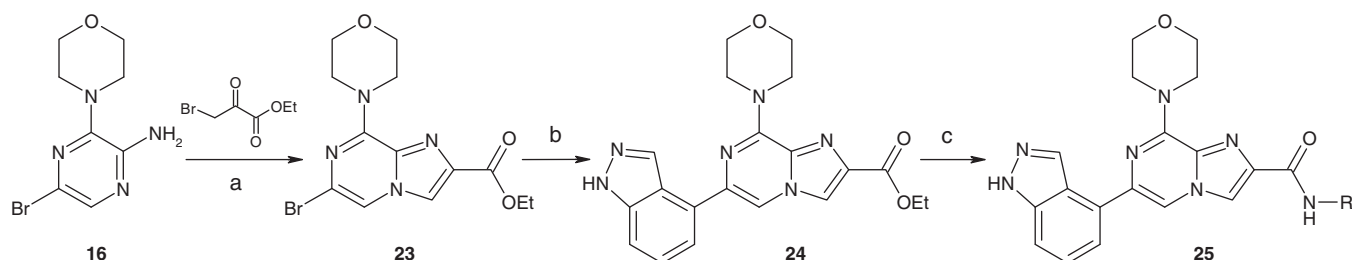
potency. Modulation of the PI3K pathway with these inhibitors was confirmed by inhibition of AKT phosphorylation on S473 in U2OS cell line, displaying compound **19** an EC<sub>50</sub> of 93 nM (Table 2).

The lower activity of **19** versus GDC-0941 could be explained by the influence of geometric (thieno-ring versus imidazo-ring) and/or electronic factors of the imidazo[1,2-*a*]pyrazine scaffold. The overlapping of both compounds (Fig. 3), using docking studies and the active conformation of GDC-0941 from X-ray structural data reflects some differences in the orientation of the 4-methanesulfonyl-piperazin-1-yl-methyl side chain.<sup>25,32</sup> This fragment in Genentech's compound is packed against the side chain of Met804 and the oxygen atoms of the sulfonyl group positioned in H-bonding distance with the side chain of Lys802 and the amide nitrogen of Ala805. However, **19** only display potential interactions with Lys802, which could explain the weaker activity observed for the imidazopyrazine inhibitor.

As a continuation of the hit to lead exploration, we prepared a series of secondary amide derivatives at the C<sub>2</sub> position. The synthesis of these imidazo[1,2-*a*]pyrazines is represented in Scheme 2 and starts with pyrazine **16**, which was refluxed with ethyl bromopyruvate in a minimum amount of DME to give compound **23**. Suzuki–Miyaura cross coupling of **23** with indazole-4-boronic acid afforded the ester precursor **24** for the final amidation reaction, which was carried out under Me<sub>3</sub>Al conditions to give amides **25** in moderated yields.

Selected results from this exploration are summarized in Table 3. Compounds with polar groups in the amide side chain **25d–h** were more potent than compound **19**, with IC<sub>50</sub> values below 50 nM. More simple amides **25a–c** were 2-fold less actives (IC<sub>50</sub> ~100 nM). Despite of the good biochemical activity, the cellular potency was rather disappointing for some of these amides (**25d–f**). This could be due to the presence of a basic side chain, which seems to be detrimental for cell membrane permeability.<sup>33</sup> Nevertheless compounds **25a**, **25g**, **25h** demonstrated a good cellular activity with values below 200 nM in U2OS cell line for the inhibition of phosphorylation of S473 residue of AKT.

Selected imidazo[1,2-*a*]pyrazine inhibitors were evaluated against the PI3K isoform family and *K*<sub>iapp</sub> data are presented in Table 4 for the four different isoforms. It is interesting to note that imidazo [1,2-*a*] pyrazine scaffold seems to give a more selectivity behaviour in terms of isoforms profile when compared to the GDC-0941, reported as modest selective PI3K $\alpha\delta$  inhibitor.<sup>25</sup> Our compounds showed a slight increase of potency against p110 $\delta$  than towards p110 $\alpha$ , about 2–10 fold, while displaying good levels of selectivity against p110 $\beta$  and p110 $\gamma$  (*K*<sub>iapp</sub> >500 nM). This activity against PI3K $\delta$  isoform can have benefits in some specific type of cancers as we mentioned previously. In this regard there are two selective PI3K $\delta$  inhibitors in clinical phases, under evaluation for haematological malignancies.<sup>34</sup>



**Scheme 2.** Reagents and conditions: (a) 1,2-DME, reflux 20 h, 35%; (b) PdCl<sub>2</sub>(dppf)/DCM, aq. K<sub>2</sub>CO<sub>3</sub>, indazole-4-boronic acid hydrochloride, DME, 130 °C, 75%; (c) Amine, Me<sub>3</sub>Al, EtOH, reflux, 6–41%.

**Table 3**  
Inhibition of PI3K $\alpha$  and phosphorylation of AKT by imidazo[1,2-*a*]pyrazine derivatives<sup>a</sup>

Compound	R	PI3K(p110 $\alpha$ ) IC <sub>50</sub> , $\mu$ M	pAKT EC <sub>50</sub> , $\mu$ M
<b>25a</b>	H	0.107 $\pm$ 0.011	0.138 $\pm$ 0.027
<b>25b</b>	Me	0.110 $\pm$ 0.022	0.600 $\pm$ 0.187
<b>25c</b>	Et	0.092 $\pm$ 0.016	0.713 $\pm$ 0.198
<b>25d</b>		0.038 $\pm$ 0.006	0.452 $\pm$ 0.068
<b>25e</b>		0.035 $\pm$ 0.008	0.429 $\pm$ 0.131
<b>25f</b>		0.035 $\pm$ 0.014	0.976 $\pm$ 0.201
<b>25g</b>		0.050 $\pm$ 0.006	0.200 $\pm$ 0.037
<b>25h</b>		0.031 $\pm$ 0.009	0.114 $\pm$ 0.039

<sup>a</sup> The values are averages of two independent experiments performed in duplicate  $\pm$  Standard Deviation. Assay conditions are described in Ref. 37,38.

**Table 4**  
mTOR activity and Biochemical selectivity profile<sup>a</sup>

Compound	mTOR IC <sub>50</sub> ( $\mu$ M)	p110 $\alpha$ K <sub>iapp</sub> (nM)	p110 $\beta$ K <sub>iapp</sub> (nM)	p110 $\delta$ K <sub>iapp</sub> (nM)	p110 $\gamma$ K <sub>iapp</sub> (nM)
<b>19</b>	>10	181 $\pm$ 13	>500	29 $\pm$ 2	>500
<b>20</b>	>10	86 $\pm$ 14	>500	8 $\pm$ 0.8	>500
<b>21</b>	>10	410 $\pm$ 50	>500	43 $\pm$ 3	>500
<b>22</b>	>10	210 $\pm$ 38	>500	65 $\pm$ 4	>500
<b>25b</b>	>10	102 $\pm$ 8	>500	17.1 $\pm$ 1	>500
<b>25d</b>	>10	65 $\pm$ 5	>500	6.5 $\pm$ 0.5	>500
<b>25e</b>	>10	44 $\pm$ 5	>500	3.6 $\pm$ 0.4	>500
<b>25h</b>	>10	60 $\pm$ 5	>500	2.8 $\pm$ 0.3	>500

<sup>a</sup> Isoforms values in the table correspond to K<sub>iapp</sub> (nM)  $\pm$  Standard Error. Assay conditions are described in Ref. 39,40.

**Table 5**  
ADME profile

Compound	human Metabolic stability <sup>a</sup> (%)	mouse Metabolic stability <sup>a</sup> (%)	CYPs inhibition <sup>b</sup> (%)	hERG binding IC <sub>50</sub> ( $\mu$ M)
<b>GDC-941</b>	54	45	<25	64
<b>19</b>	48	32	<25	100
<b>22</b>	35	28	<25	
<b>25g</b>	75	62	<25	

<sup>a</sup> Percent remaining after 30 min incubation of 1  $\mu$ M compound with 0.7 mg/ml human/mouse liver microsomes. Assays performed at Wuxi in duplicates.

<sup>b</sup> Percent of CYPs inhibition at 10  $\mu$ M test compound. Assays performed at Wuxi in duplicates (CYPs panel: 1A2, 2C9, 2C19, 2D6, 3A4).

Representative PI3K inhibitors were tested against mTOR (mammalian Target of Rapamycin),<sup>40</sup> a member of PI3K class IV, displaying high selectivity (IC<sub>50</sub> >10.0  $\mu$ M, Table 4). GDC-0941 was included in our studies<sup>36</sup> showing an IC<sub>50</sub> = 0.42  $\mu$ M for mTOR inhibition (reported in literature K<sub>iapp</sub> = 0.58  $\mu$ M).<sup>25</sup> The use of imidazo [1,2-*a*] pyrazine scaffold confers higher selectivity to these compounds versus mTOR kinase. Compounds were also tested in a 24 kinase panel<sup>35</sup> showing a good selectivity profile, with values under 50% of inhibition at 5–10  $\mu$ M.

In Table 5 is presented preliminary in vitro ADME data generated for compounds **19**, **22**, **25g**. Our compounds showed minimal inhibition, less than 25%, of five of the principal cytochrome P450 isoforms, sharing similar results with GDC-0941. Metabolic stability was measured in human and mouse liver microsomes with diverse results depending on the decoration of the compounds. Compound **19** has a similar behaviour than GDC-0941 (45–54%, mouse–human, of compound remaining in our assay, and 92% reported in literature in different assay conditions).<sup>25</sup> The introduction of a chlorine atom in C<sub>5</sub> decrease the stability of compound **22**, meanwhile the opposite effect was observed with the amide **25g**. In addition, there was no significant blockade of the hERG channel for compound **19** (IC<sub>50</sub> = 100  $\mu$ M) in the Herg binding assay.<sup>41</sup>

In summary, we have discovered novel PI3K inhibitors by ligand based rational design. The series of 8-morpholinyl-imidazo[1,2-*a*]pyrazines afforded potent compounds against PI3K $\delta$  and  $\alpha$

isoforms, showing downregulation of inhibition of AKT<sup>S473</sup> phosphorylation in a U2OS cell line. These compounds show also an improved selectivity vs mTOR kinase. Available data justifies additional optimization of this chemical series and progress in this direction shall be reported in due course.

## Acknowledgments

This research was supported by the Ministry of Science and Innovation (MICINN) of Spain through the project CIT-090100-2007-48.

We thank Elena Cendón and Antonio Salgado for compound purification and characterization. We also thank Isabel Reymundo and Genoveva Mateos for compound handling and sample preparation and Manuel Urbano for data management.

## References and notes

- Leevers, S. J.; Vanhaesebroeck, B.; Waterfield, M. D. *Curr. Opin. Cell Biol.* **1999**, *11*, 219.
- Lawlor, M. A.; Alessi, D. R. *J. Cell Sci.* **2001**, *114*, 2903.
- Vanhaesebroeck, B.; Leevers, S. J.; Ahmadi, K.; Timms, J.; Katso, R.; Driscoll, P. C.; Woscholski, R.; Parker, P. J.; Waterfield, M. D. *Annu. Rev. Biochem.* **2001**, *70*, 535.
- Cantley, L. C. *Science* **2002**, *296*, 1655.
- Domin, J.; Waterfield, M. D. *FEBS Lett.* **1997**, *410*, 91.
- Vanhaesebroeck, B.; Waterfield, M. D. *Exp. Cell Res.* **1999**, *253*, 239.
- Vanhaesebroeck, B.; Leevers, S. J.; Panayotou, G.; Waterfield, M. D. *Trends Biochem. Sci.* **1997**, *22*, 267.
- Fruman, D. A.; Meyers, R. E.; Cantley, L. C. *Annu. Rev. Biochem.* **1998**, *67*, 481.
- Vivanco, I.; Sawyers, C. L. *Nat. Rev. Cancer* **2002**, *2*, 489.
- Katso, R.; Okkenhaug, K.; Ahmadi, K., et al. *Annu. Rev. Cell Dev. Biol.* **2001**, *17*, 615.
- Wymann, M. P.; Zvelebil, M.; Laffargue, M. *Trends Pharmacol. Sci.* **2003**, *24*, 366.
- Liu, P.; Cheng, H.; Roberts, T. M.; Zhao, J. J. *Nat. Rev. Drug Disc.* **2009**, *8*, 627.
- Ali, I. U.; Schriml, L. M.; Dean, M. J. *Natl. Cancer Inst.* **1992**, *1999*, 91.
- Cross, D. A.; Alessi, D. R.; Cohen, P., et al. *Nature* **1995**, *378*, 785.
- Samuels, Y.; Wang, Z.; Bardelli, A.; Silliman, N.; Ptak, J.; Szabo, S.; Yan, H.; Gazdar, A.; Powell, S. M.; Riggins, G. J.; Willson, J. K.; Markowitz, S.; Kinzler, K. W.; Vogelstein, B.; Velculescu, V. E. *Science* **2004**, *304*, 554; Leslie, N. R.; Downes, C. B. *Biochem. J.* **2004**, *382*, 1.
- Shayesteh, L.; Lu, Y.; Kuo, W.-L.; Baldocchi, R.; Godfrey, T.; Collins, C.; Pinkel, D.; Powell, B.; Mills, G. B.; Gray, J. W. *Nat. Genet.* **1999**, *21*, 99.
- Ma, Y.-Y.; Wei, S.-J.; Lin, Y.-C.; Lung, J.-C.; Chang, T.-C.; Whang-Peng, J.; Liu, J. M.; Yang, D.-M.; Yang, W. K.; Schen, C.-Y. *Oncogene* **2000**, *19*, 2739.
- Parsons, D. W.; Wang, T.-L.; Samuels, Y.; Bardelli, A.; Cummins, J. M.; DeLong, L.; Silliman, N.; Ptak, J.; Szabo, S.; Willson, J. K.; Markowitz, S.; Kinzler, K. W.; Vogelstein, B.; Lengauer, C.; Velculescu, V. E. *Nature* **2005**, *436*, 792.
- Campbell, I. G.; Russell, S. E.; Choong, D. Y.; Montgomery, K. G.; Ciavarella, M. L.; Hooi, C. S.; Cristiano, B. E.; Pearson, R. B.; Phillips, W. A. *Cancer Res.* **2004**, *64*, 7678.
- Kang, S.; Bader, A. G.; Vogt, P. K. *Proc. Natl. Sci. U.S.A.* **2005**, *102*, 802.
- Jia, S.; Liu, Z.; Zhang, S.; Liu, P.; Zhang, L.; Lee, S. H.; Zhang, J.; Signoretti, S.; Loda, M.; Roberts, T. M.; Zhao, J. J. *Nature* **2008**, *454*, 776.
- Kok, K.; Nock, G. E.; Verrall, E. A.; Mitchell, M. P.; Hommes, D. W.; Peppenlenbosch, M. P.; Vanhaesebroeck, B. *PLoS One* **2009**, *4*, e5145.
- Sujobert, P.; Bardet, V.; Cornillet-Lefebvre, P.; Hayflick, J. S.; Prie, N.; Verdier, F.; Vanhaesebroeck, B.; Muller, O.; Pesce, F.; Ifrah, N.; Hunault-Berger, M. *Blood* **2005**, *106*, 1063.
- Burger, M. T.; Pecchi, S.; Wagman, A.; Ni, Z.; Knapp, M.; Hendrickson, T.; Atallah, G.; Pfister, K.; Zhang, Y.; Bartulis, S.; Frazier, K.; Ng, S.; Smith, A.; Verhagen, J.; Haznedar, J.; Huh, K.; Iwanowicz, E.; Xin, X.; Menezes, D.; Merritt, H.; Lee, I.; Wiesmann, M.; Kaufman, S.; Crawford, K.; Chin, M.; Bussiere, D.; Shoemaker, K.; Zaror, I.; Maira, S.; Voliva, C. F. *ACS Med. Chem. Lett.* **2011**, *2*(10), 774.
- Folkes, A. J.; Ahmadi, K.; Alderton, W. K.; Alix, S.; Baker, S. J.; Box, G.; Chuckowree, I. S.; Clarke, P. A.; Depledge, P.; Eccles, S. A.; Friedman, L. S.; Hayes, A.; Hancox, T. C.; Kugendradas, A.; Lensun, L.; Moore, P.; Olivero, A. G.; Pang, J.; Patel, S.; Pergl-wilson, G. H.; Raynaud, F. I.; Robson, A.; Saghir, N.; Salphati, L.; Sohal, S.; Ultsch, M. H.; Valenti, M.; Wallweber, H. J. A.; Wan, N. C.; Wiesmann, C.; Workman, P.; Zhyvoloup, A.; Zvelebil, M. J.; Shuttleworth, S. J. *J. Med. Chem.* **2008**, *51*, 5522.
- Link, W.; Oyarzabal, J.; Serelde, B. G.; Albarrán, M. I.; Rabal, O.; Cebria, A.; Alfonso, P.; Fominaya, J.; Renner, O.; Peregrino, S.; Soilán, D.; Ceballos, P. A.; Hernández, A. I.; Lorenzo, M.; Pevarello, P.; Granda, T. G.; Kurz, G.; Carnero, A.; Bischoff, J. R. *J. Biol. Chem.* **2009**, *284*, 28392.
- Hayakawa, M.; Kaizawa, H.; Moritomo, H.; Koizumi, T.; Ohishi, T.; Okada, M.; Ohta, M.; Tsukamoto, S.; Parker, P.; Workman, P.; Waterfield, M. *Bioorg. Med. Chem.* **2006**, *14*, 6847.
- Hayakawa, M.; Kaizawa, H.; Moritomo, H.; Koizumi, T.; Ohishi, T.; Yamano, M.; Okada, M.; Ohta, M.; Tsukamoto, S.; Raynaud, F. I.; Workman, P.; Waterfield, M. D.; Parker, P. *Bioorg. Med. Chem. Lett.* **2007**, *17*, 2438.
- As far as we know, 93 patents reported PI3K inhibitors with 'mopholinyl pyrimidine' core.
- Walker, E. H.; Pacold, M. E.; Perisic, O. *Mol. Cell* **2000**, *6*, 909.
- Knight, Z. A.; Chiang, G. G.; Alaimo, P. G.; Kenski, D. M.; Ho, C. B.; Coan, K.; Abraham, R. T.; Shokat, K. M. *Bioorg. Med. Chem.* **2004**, *12*, 4749.
- For docking purposes, the protein used was obtained from the crystal of the PI3K gamma in complex with GDC-0941 (3DBS). Program used was GOLD3.1 from Open Eye Scientific Software.
- Permeability of some compounds was measured in MDCK cells. Results showed that compounds with basic amines (**25d**, **25e**) had lower permeability (Paap <1) than compounds **25a**, **25b**, **25g** with Paap >3.5, where Paap denotes the apparent permeability coefficient.
- Norman, P. *Expert Opin. Ther. Patents* **2011**, *21*, 1773.
- Panel of 24 kinases: AKT1, ARK5, BRAF-V600E, CK1α1, DYRK1A, EGF-R, FAK, FGF-R1, FLT3, IGF1-R, IKKβ, INS-R, JAK2, JNK1, KIT, MEK1, MET, MST1, PAK1, PDGFR, PIM1, PIM2, RPS6KA1, SGK1.
- GDC-0941 was purchased to Chemexpress (MFCD11616196).
- The PI3Kα activity was measured by using the commercial ADP Hunter™ Plus assay available from DiscoverX, homogeneous assay to measure the accumulation of ADP, a universal product of kinase activity. The enzyme, PI3K (p110α/p85α) was purchased from Carna Biosciences and the assay was done following the manufacturer recommendation with slight modifications in the kinase buffer (50 mM HEPES, pH 7.5, 3 mM MgCl<sub>2</sub>, 100 mM NaCl, 1 mM EGTA, 0.04% CHAPS, 2 mM TCEP and 0.01 mg/ml BGG), and working at 10 nM PI3Kα (p110α/p85α) and at 50 μM of ATP concentration. Values were plotted against the inhibitor concentration and fitted to a sigmoid dose-response curve by using GraphPad Prism version 5.03 (GraphPad Software CA, USA). Values given are averages of two independent experiments performed in duplicate.
- Cellular activity was measured as endogenous levels of phospho-Akt1 (Ser473) protein after serum stimulation in U2OS (osteosarcoma) cells growing in 0.1 % of FBS. Assay was run under C-Elisa format (Reagent: Supersignal Elisa Femto, purchased from Pierce). Values were plotted against the inhibitor concentration and fitted to a sigmoid dose-response curve using GraphPad Software.
- The kinase activity of PI3K isoforms was measured by using the commercial PI3-kinase (h) HTRF™ assay available from Millipore, following the manufacturer recommendations. PI3Kα (p110α/p85α) and PI3Kδ (p110δ/p85α) were used at 100 pM; PI3Kβ (p110β/p85α) and PI3Kγ isoforms (p110γ) at 500 pM and 4 nM respectively. ATP concentration was 50 times KMATP: 200 μM for PI3Kα and PI3Kδ, 250 μM for PI3Kβ and 100 μM for PI3Kγ. PIP2 was held at 10 μM. Values were normalized against the control activity included for each enzyme (i.e., 100 % PI3K activity, without compound). These values were plotted against the inhibitor concentration and were fitted to a sigmoidal dose-response (variable slope) curve by using GraphPad Software. The obtained IC<sub>50</sub> were converted to K<sub>iapp</sub> according to Cheng-Prusoff equation for competitive inhibitors (Cheng, Y.; Prusoff, W.H. *Biochem. Pharmacol.* **1973**, *22*, 3099).
- MTOR (FRAP1), LanthaScreen™ Tb-anti-p4EBP1 (phosphor-threonine 46) and GFP-4E BP1 were purchased from Invitrogen. Reaction conditions used were those recommended by the manufacturer. Values given are averages of two independent experiments performed in duplicate.
- hERG membrane radioligand binding assay. CHO-K1 cell line stably expressing hERG channel, radioligand: [<sup>3</sup>H]-astemizole. Assays performed at Wuxi in duplicates.